Aerosol Res., 3, 205–218, 2025
https://doi.org/10.5194/ar-3-205-2025

AEROSOL Research
Open Access

Emission dynamics of reactive oxygen species and oxidative potential in particles from a petrol car and wood stove

Battist Utinger[1,★], Alexandre Barth[1,★], Andreas Paul[2], Arya Mukherjee[3], Steven John Campbell[4], Christa-Maria Müller[1], Mika Ihalainen[3], Pasi Yli-Pirilä[3], Miika Kortelainen[3], Zheng Fang[5], Patrick Martens[6,a], Markus Somero[3], Juho Louhisalmi[3], Thorsten Hohaus[2], Hendryk Czech[6,7], Olli Sippula[3,8], Yinon Rudich[5], Ralf Zimmermann[6,7], and Markus Kalberer[1]

[1]Department of Environmental Science, University of Basel, Basel, Switzerland
[2]IEK-8 Troposphere, Forschungszentrum Jülich GmbH, Jülich, Germany
[3]Department of Environmental and Biological Science, University of Eastern Finland, Kuopio, Finland
[4]MRC Centre for Environment and Health, Environmental Research Group, Imperial College London, London, UK
[5]Department of Earth and Planetary Science, Weizmann Institute of Science, Rehovot, Israel
[6]Department of Technical and Analytical Chemistry, University of Rostock, Rostock, Germany
[7]Comprehensive Molecular Analytics, Helmholtz Centre Munich, Munich, Germany
[8]Department of Chemistry, University of Eastern Finland, Joensuu, Finland
[a]now at: Desert Research Institute, Reno, NV 89512, USA
★These authors contributed equally to this work.

Correspondence: Markus Kalberer (markus.kalberer@unibas.ch)

Received: 7 October 2024 – Discussion started: 15 October 2024
Revised: 30 January 2025 – Accepted: 12 March 2025 – Published: 22 April 2025

Abstract. Air pollution is one of the largest environmental health risks and one of the leading causes of adverse health outcomes and mortality worldwide. The possible importance of the oxidative potential (OP) as a metric to quantify particle toxicity in air pollution is increasingly being recognised. In this work, the OP and reactive oxygen species (ROS) activity of particles from fresh and aged petrol passenger car emissions and residential wood combustion (RWC) emissions were investigated using two novel instruments. Applying online instruments using an ascorbic acid (AA) and 2′,7′-dichlorodihydrofluorescein (DCFH) assay provides a much higher temporal resolution compared with traditional filter-based methods and allows for new insights into the highly dynamic changes in the OP and ROS activity of these sources. Due to the efficiency of the particulate filter in the Euro 6d car, almost no primary particles were emitted and, thus, no particle OP or ROS activity was detected in primary exhaust. However, a substantial and highly dynamic OP and ROSs were observed after photochemical ageing due to the formation of secondary particles. Increasing OP and ROS activity due to ageing was also observed when comparing fresh and aged RWC emissions. Overall, RWC emissions had higher OP and ROS signals compared with car emissions. This suggests that aged RWC emissions could be a major contributor to air pollution toxicity and may be an intrinsically more harmful emission source than car exhaust, although the formation potential for secondary particles from car emissions was still high. These measurements illustrate the strong differences and highly dynamic nature of toxicity-relevant particle properties from two air pollution sources and could contribute to more efficient air pollution mitigation policies.

Published by Copernicus Publications on behalf of the European Aerosol Assembly (EAA).

1 Introduction

Air pollution is a complex mixture of gaseous compounds and aerosol particles composed of both natural and anthropogenic constituents, with common anthropogenic sources including fossil fuel combustion, non-exhaust traffic emissions, industrial processes, and agricultural activities. The specific composition and concentration of pollutants in the ambient air varies depending on a range of factors like local sources and meteorological conditions. According to numerous epidemiological studies, there is a compelling association between air pollution and various health effects (Hart et al., 2015; Laden et al., 2006; Lepeule et al., 2012). Elevated levels of ambient aerosol particles have been associated with increased hospital admissions and deaths from a variety of diseases, including cancer, respiratory illness, and cardiovascular disease (Baulig et al., 2003; Donaldson et al., 2001; Li et al., 2003; Offer et al., 2022; Prahalad et al., 2001). In a recent report, the World Health Organization (WHO) has recognised that air pollution and, specifically, aerosol particles are the single largest environmental threat to human health (World Health Organization, 2021). Despite strong evidence linking air pollution particles and negative health outcomes, the specific mechanisms and properties by which aerosol particles cause these effects are poorly understood. Identifying the health-relevant particle properties, including the most damaging chemical components and their emission sources, will allow for the development of more effective strategies to minimise exposure from the most harmful sources (Brunekreef and Holgate, 2002; Künzi et al., 2015). Current guidelines and legal regulations mainly address total particle mass concentration as the criterion to evaluate air quality. However, there is proof that differences in the chemical composition of particulate matter (PM) play a role in its toxicity (Kelly and Fussell, 2012). There is also increasing evidence that oxidising particle components might play a role in particle toxicity (Øvrevik et al., 2015).

Reactive oxygen species (ROSs) are highly reactive oxygen-containing molecules and radicals such as hydrogen peroxide, hydroxyl radical, superoxide, and organic peroxides and are formed in oxidation reactions in the atmosphere. These can be delivered exogenously through particle exposure (especially larger, less-volatile organic peroxides and radicals) or can be produced endogenously when particles are deposited on the lung surface after inhalation (such as hydroxyl radical or superoxide) (Campbell et al., 2019). Exogenous reactive species also exist in the gas phase; however, in this study, we focus on particle exposure only. Another potential metric serving as proxy for particle toxicity is the oxidative potential (OP) of particles, which is defined as the ability of aerosol particle components to generate ROSs inside the body and, simultaneously, deplete antioxidants (Kelly, 2003). The exceedance of the body's antioxidative capacity can lead to oxidative stress, which has been linked to negative health effects (Pizzino et al., 2017). In recent years, the importance of the OP and ROSs in air pollution research has gained increasing attention, as these parameters might play a major role in PM-induced diseases (Guascito et al., 2023). For example, the European parliament recently adopted a revised Ambient Air Quality Directive for Europe (Council of the European Union, 2024). It suggests the expansion of monitored pollutants at supersites to also include the OP among other pollutants of emerging concern next to the standard network of measurements (Council of the European Union, 2024).

Traditionally, ROS and OP measurements have been based on the collection of PM filters and subsequent laboratory analysis. However, the time lag between sample collection and analysis can be long, potentially leading to a severe underestimation of the PM OP due to the instability and, therefore, short lifetime of ROSs. Recent studies have shown that only a minor fraction (1 %–40 %) of particle-bound ROSs in organic aerosol collected on filters is stable on a timescale of up to a week compared with direct-to-reagent online measurements, emphasising the need for the immediate analysis of particles for accurate quantification of ROSs and the OP (Campbell et al., 2023; Zhang et al., 2022). Other studies have also shown short half-lives of compounds contributing to ROSs and the OP in aerosol particles, such as radicals (Campbell et al., 2019), peroxy acids (Steimer et al., 2018), and hydroperoxides (Zhao et al., 2018), that range from minutes to hours. These findings indicate that online measurement methods that utilise a direct-to-reagent sampling approach are required for robust quantification of the OP and ROSs, particularly to capture the short-lived reactive components.

PM originating from anthropogenic sources typically has a higher OP than natural emissions, as evidenced by a recent study which observed an OP that was a factor of 3 higher for anthropogenic compared with biogenic secondary organic aerosol (SOA) (Daellenbach et al., 2020; Zhang et al., 2022). Two important classes of anthropogenic aerosols are emissions from residential wood combustion (RWC) and traffic emissions. The anthropogenic contribution from RWC is especially visible during winter, when most of the $PM_{2.5}$ (particles with a diameter of less than 2.5 µm) comes from biomass burning (Denier van der Gon et al., 2015). Even at very low ambient concentrations of PM attributed to RWC, there is an observable health impact. A recent study estimated that annual concentrations of RWC aerosol as low as $0.46\,\mu g\,m^{-3}$ can lead to a decrease in life expectancy of 0.1 years (Orru et al., 2022). Additionally, emissions from road traffic are a major source of urban air pollution. While modern exhaust treatment systems can reduce primary emissions of PM, the formation potential of secondary emissions is still high, even with engines complying to the newest regulations (Gao et al., 2021; Hartikainen et al., 2023; Platt et al., 2017).

Recent studies have attempted to uncover the relationship between the composition and potential biological effects of PM (Campbell et al., 2024). The OP has emerged as a

novel and biologically significant chemical metric that may serve as a critical connection between the chemical composition of particles and their associated adverse health effects (Bates et al., 2019). Specific components like organic/elemental carbon and metals were associated with an increased risk of negative health outcomes (Atkinson et al., 2015; Heo et al., 2014). Thus, the composition of aerosol particles and their emission sources play a key role in dictating the OP and ROS formation. The sources and components that influence the OP in the complex ambient aerosol are currently poorly understood, but this knowledge would provide crucial information for policymakers to more efficiently abate air pollution.

In this study, we address this knowledge gap and quantify, for the first time, the highly dynamic particulate OP and ROS characteristics of emissions of a petrol passenger car as well as of a residential wood stove. Two recently developed online instruments were used in this study that allow for unprecedented high-temporal-resolution (10 min) OP and ROS measurements: the online oxidative potential ascorbic acid instrument (OOPAAI) measures the aerosol particle OP using an online ascorbic acid assay (Utinger et al., 2023) and the online particle-bound ROS instrument (OPROSI) quantifies particle-bound ROSs (Wragg et al., 2016). Besides sampling the emissions directly (i.e. primary emissions), they were also passed through a photochemical flow tube reactor to simulate two different atmospheric ageing conditions. Combustion conditions have highly dynamic emission profiles, and only online instruments, as used in this study, are able to characterise the fast-changing OP and ROS properties of particle emissions. Furthermore, we calculated, for the first time, emission factors (EFs) for the OP (EF_{OP}) and ROSs (EF_{ROS}), thereby enabling the assessment of health risks associated with exposure to PM emitted from these two sources and providing information on a potential link between the atmospheric ageing of particles and oxidative stress.

2 Material and methods

2.1 Reagents

All of the following chemicals were obtained from Sigma-Aldrich and were used without further purification unless otherwise indicated: ascorbic acid (AA, 99.0 %), dehydroascorbic acid (DHA, 99.0 %), hydrochloric acid (HCl, 0.1 M) sodium hydroxide (NaOH, 0.1 M) solution, Chelex 100 sodium form, *o*-phenylenediamine (OPDA, $\geq$ 99.5 %), 4-(2-hydroxyethyl)-1-piperazineethanesulfonic acid (HEPES, $\geq$ 99 %), methanol (99.9 %), peroxidase from horseradish (Type VI, HRP), 2,7-dichlorofluorescin diacetate (DCFH-DA, 97 %), 3 % hydrogen peroxide solution, phosphate-buffered saline solution (PBS, 1 M), zero-grade air (Model 737–250, Aadco Instruments Inc., USA), and N_2 gas (99.999 %, Linde, Finland).

2.2 Aerosol generation and characterisation

Here, only a brief overview of the experimental set-up of emission generation, ageing, and sampling is given. More details can be found in Mukherjee et al. (2024) and Paul et al. (2024). Figure 1 illustrates a simplified schematic of the experimental set-up. The raw exhaust was sampled directly at the tail pipe of a EURO 6d petrol car (Škoda Scala 2021) or the chimney of a residential wood stove (Aduro 9.3). Flowing through a heated sampling line, a two-step dilution system reduced the concentration and temperature of the sample using a porous tube and an ejection diluter. The dilution ratio was set at 1 : 17 during the car emission experiments and at 1 : 60 during the RWC experiments because of the large difference in PM and gas-phase concentrations of the two PM sources and to ensure a final maximal PM concentration of between 500 and 2000 $\mu g\,m^{-3}$ (Figs. 2, 5). The exhaust flow then passed through the photochemical emission ageing flow tube reactor (PEAR) to simulate atmospheric ageing (Ihalainen et al., 2019). For primary experiments, the PEAR was not in operation, but the aerosol was passed through it nonetheless to have comparable results. The equivalent photochemical ages were determined to be between 1.1 and 5.1 d by determining the decay kinetics of fully deuterated butanol measured by a proton-transfer-reaction time-of-flight mass spectrometer (PTR-TOF-MS 8000, IONICON) (Paul et al., 2024; Schneider et al., 2024). Furthermore, a scanning mobility particle sizer (SMPS, Model 3776 CPC, Model 3080 classifier, TSI) and low-pressure impactor mass measurements (ELPI, Dekati Ltd.) were used to quantify the particle number size distributions. The OOPAAI and OPROSI were connected after the PEAR to measure the OP and ROSs from both primary and secondary emissions. Primary emissions without oxidative ageing by the PEAR were measured as well, to allow for a comparison between primary and aged combustion particles. Due to high particle concentrations during the RWC experiments, an additional porous tube diluter was connected and set to a dilution ratio of 1 : 1.5 to 1 : 3, depending on experimental conditions. By passing the sample through a high-efficiency particle-arresting (HEPA) filter (HEPA-CAP150, Whatman), blank measurements were possible during experiments to check for background drifts or gas-phase artefacts. Subsequently, two 1 m long home-built denuders filled with activated charcoal (untreated, granular, Sigma-Aldrich) as well as one denuder with eight honeycomb-shaped charcoal elements (IONICON) were connected in-line to remove any reactive gas-phase components that could contribute to the online ROS or OP signals (e.g. O_3 or oxidising volatile organic compounds). The charcoal was regenerated at 230 °C for 24 h every second day. Having both instruments connected to the same denuders allowed for a higher sample flow through them, reducing particle losses, which were estimated to be 10 %; thus, the data were corrected by 10 % (Fig. S1 in the Supplement).

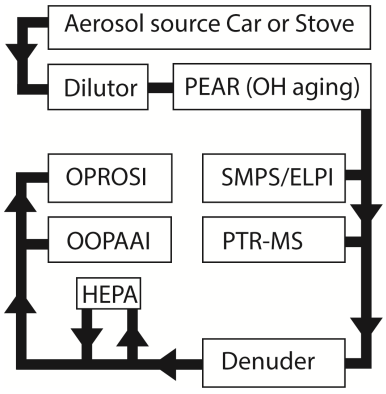

Figure 1. A simplified schematic of the components and analysis instruments relevant for this paper. On its way from the emission source to the PEAR chamber, the aerosol undergoes a first dilution step before a second dilution and the removal of the reactive gas-phase component are applied.

The car was operated following a driving cycle. One cycle lasted for 1 h, and an experiment consisted of four cycles, resulting in 4 h measurement periods. Every cycle consisted of four different steady-state driving conditions starting with 5 min of idling; followed by 15 min of 50 km h^{-1} (fourth gear), 15 min of 100 km h^{-1} (fifth gear), and 15 min of 80 km h^{-1} (fifth gear), respectively; and ending with 10 min of idling. For the RWC measurements, an initial batch of beech wood logs (1.85 kg) with 150 g of beech kindling was ignited. Similar procedures have been used in other studies employing the same stove (Ihantola et al., 2022; Leskinen et al., 2023; Martens et al., 2021). After every 35 min, an additional batch of 2 kg of beech logs was added for a total of six batches. After the last addition, the wood was left to burn out (ember phase) for 30 min, during which the supply of fresh air was stopped. One RWC experiment lasted 4 h. Blank OP and ROS measurements were performed before and after the experiments as well as at different time points during the experiment to characterise potential gas-phase contributions, denuder efficiency, and instrument backgrounds. The OOPAAI was started the day before an experiment day, and blank measurements were run overnight to ensure a stable blank. The OPROSI was started only 1 h before the start of an experiment due to the higher costs for chemicals and a faster stable blank. The cellulose grade-1 filters inside the liquid systems of both instruments, which remove insoluble particles, were changed daily to avoid excessive contamination by insoluble particles (see Sect. 3.2 for further details). Additionally, this was done between each 4 h run of the RWC experiments for the OPROSI. The OOPAAI and OPROSI were calibrated once a week to ensure consistent performance for the duration of the measurement campaign, as described in Wragg et al. (2016) and Utinger et al. (2023).

2.3 Chemical preparation

All chemical solutions used in this study were made immediately prior to measurements, except where otherwise specified. Water used to prepare the solutions was purified by a high-purification water unit (resistivity 18.2 MΩ cm^{-1}). For the ascorbic acid assay, the water was passed through a fritted column filled with 100 g of Chelex 100 resin, to further reduce the amount of contamination. The valve was adjusted to a flow of one drop per minute through the resin. The treatment was used to remove trace metals (i.e. copper and iron) to avoid interference with the AA oxidation caused by the sample. A 200 mM HEPES buffer stock solution, to adjust the pH to a physiologically relevant range (pH 6.8), was prepared monthly using Chelex-treated water and was stored at 4 °C. HEPES was used because it has a lower chelating effect of transition metals than PBS (Utinger et al., 2023). AA solutions were prepared the day before the experiments in an effort to stabilise the background drift caused by the auto-oxidation of AA. A total of 8.8 mg of AA was dissolved in 25 mL of HEPES stock solution and 225 mL of Chelex-treated water to form a 200 µM AA working solution. OPDA solution was prepared by dissolving 0.54 g of OPDA in 250 mL of 0.1 M hydrochloric acid to form a 20 mM working solution. For the ROS measurements of the DCFH assay, the HRP stock solution was prepared weekly by dissolving 5000 units in 500 mL of water and was stored at 4 °C. HRP working solution was prepared using 100 mL of HRP stock solution, 100 mL of 1 M PBS, and 800 mL of pure water. DCFH-DA stock solution was prepared weekly by dissolving 50 mg of DCFH-DA in 50 mL of methanol and sonicating it for 15 s and was stored at −20 °C. DCFH working solution was prepared by reacting 4 mL of 0.1 M NaOH with 4.872 mL of the DCFH-DA stock solution for 30 min in the dark. Subsequently, 100 mL of 1 M PBS and pure water were added to a total volume of 1 L. The HRP and DCFH working solutions were prepared the night before and stored at 4 °C. For both assays, a calibration was performed once per week, as described in Utinger et al. (2023) for ascorbic acid and in Wragg et al. (2016) for DCFH, to convert the raw fluorescence signal to the corresponding equivalents using known concentrations of DHA and H_2O_2.

2.4 Data analysis

The fluorescence spectroscopy data were first corrected for the blank background and its drift over the 4 h measurement period. This was done by applying a fit across all blank measurements and subtracting the fitted blank values from the raw signal. The drift was less pronounced in the OOPAAI for the car exhaust measurements, and a linear fit was sufficient. However, for the stronger drifts during the RWC measurements, the baseline was fitted using a B-spline function in OriginPro (OriginLab 2023). For the OPROSI corrections, a third-order polynomial fit was used

for the car and RWC data. The data were averaged to 10 s to match the electrical low-pressure impactor mass measurements (ELPI, Dekati Ltd.), providing total $PM_{2.5}$ mass concentrations. The ELPI particle size range used for the car measurements was $PM_{0.3}$ (particles with a diameter of less than 0.3 µm), whereas $PM_{0.6}$ (particles with a diameter of less than 0.6 µm) was used for the RWC emissions. These size ranges were chosen because gaseous ions in the exhaust gas would lead to measurement artefacts and a considerable overestimation of total PM mass in the larger size bins of the ELPI. This can be shown by the fact that no significant particle concentrations were present above these size ranges as measured by the SMPS and ELPI (Fig. S2) (Paul et al., 2024). Taking these ELPI size bins, the mass concentrations were in a similar range to those measured by the SMPS, while still offering a higher temporal resolution (Fig. S3). A constant particle density of 1.6 g cm^{-3} was used for mass calculations of the car measurements (Paul et al., 2024), whereas densities from Mukherjee et al. (2024) were used for PM emitted by the stove. Average PM density values of 1.5, 1.75, and 1.85 g cm^{-3} during the flaming and residual burning phases were used for fresh, short-term ageing, and medium-term ageing measurements, respectively. The methods to derive ROS and OP EFs for car exhaust and for RWC PM are described and derived in Paul et al. (2024) and Reda et al. (2015), respectively, and calculated as shown in the following equation:

$$\mathrm{EF} = \frac{\text{nmol ROSs}}{\text{kg fuel}} = \frac{\text{mg aerosol}}{\text{kg fuel}} \times \frac{\text{nmol ROSs}}{\text{mg aerosol}}.$$

3 Results and discussion

The OP and ROS concentrations of tail pipe particle emissions from a EURO 6d petrol car and from beech wood combustion using a residential wood stove were quantified. Fresh emissions were characterised, and changes in chemical properties caused by photochemical ageing in a flow tube reactor were also studied. The OP and ROS results are presented normalised to the sampled air volume (OP_V and ROS_V, respectively) as well as normalised to the PM mass (OP_M and ROS_M, respectively).

3.1 OP and ROS concentrations of primary and secondary car exhaust emissions

Four-hour experiments were performed and consisted of four 1 h driving cycles with an idling phase and three engine loads, as described in Sect. 2. Both instruments could not detect any signal for the primary exhaust (Fig. S4). As part of the EURO 6d regulations, the car's exhaust system is fitted with a petrol (gasoline) particle filter (GPF), reducing primary exhaust emissions (Paul et al., 2024). Thus, the possible particle OP and ROS activity in primary particulate emissions were below the limit of detection (LOD) of our online instruments. LOD values (in units of nmol DHA m^{-3} and nmol H_2O_2 m^{-3}, respectively) depend on the OP and ROS content of the respective particle and are, therefore, variable. For SOA, the LOD is around 5 µg m^{-3} (Utinger et al., 2023; Wragg et al., 2016), which is much lower than any of the conditions measured during this campaign where no GPF was used. In contrast, as illustrated in Fig. 2, significant OP_V and ROS_V values and particle mass ($PM_{2.5}$) were measured for photochemically aged car exhaust for an equivalent atmospheric ageing period of 2.1 d in the PEAR chamber, with OP and ROS concentrations of up to 800 nmol DHA m^{-3} and 2200 nmol H_2O_2 eq. m^{-3} being measured. Aged particle emissions consisted only of secondary organic and inorganic particles. Figure 2 clearly demonstrates that both instruments are sensitive to SOA, as has also been shown in previous studies (Utinger et al., 2023; Wragg et al., 2016), while inorganic secondary particles, mainly composed of NH_4, SO_4, and NO_3, do not react with the AA and DCFH in our online instruments (Paul et al., 2024). OP_V and ROS_V concentrations generally follow the particle mass closely, although some changes in PM mass are not reflected in OP_V and ROS_V. This shows that different engine loads not only cause a change in the total aged PM mass concentration but also in the particle OP and ROS activity. The highest mass concentrations and also OP and ROS signals were measured at 50 km h^{-1}, compared with 80 and 100 km h^{-1} where lower OP, ROS, and mass concentration values were observed. During the last cycle (Fig. 2, after 3 h), blank OP and ROS measurements were performed by removing all particles from the exhaust flow with a HEPA filter in front of the OOPAAI and OPROSI. These blank measurements clearly illustrate that gaseous components in the aged exhaust were removed efficiently by the charcoal denuders in our instruments (Fig. 1) and do not cause any measurement artefacts, as both instruments returned to blank-level values.

Two different ageing conditions were applied to investigate the potential influence of photochemical ageing on the intrinsic OP and ROS values. In Fig. 3, the averaged OP_M values of the two ageing conditions are shown. Photochemical ages of approximately 2.1 d (Fig. 3a) and 5.1 d (Fig. 3b) represent short-term and medium-term ageing processes in the atmosphere. Overall, the OP_M was similar between the two ageing times. We observed peak OP_M concentrations that were about 2 times higher during idling and at the beginning of the 50 km h^{-1} period compared with the other engine conditions, e.g. the 100 and 80 km h^{-1} loads during the short-term ageing condition (0.31 ± 0.19 nmol DHA µg^{-1} vs. 0.15 ± 0.03 nmol DHA µg^{-1}, respectively). This difference was about 40 % larger during the medium-term ageing condition (0.41 ± 0.29 nmol DHA µg^{-1} vs. 0.12 nmol DHA µg^{-1}, respectively). The idling and 50 km h^{-1} periods also show the highest variability averaged across the 15 driving cycles due to fluctuations in the emissions. Interestingly, a consistent, short 65 % increase in OP_M at the beginning of the 100 km h^{-1} condition was measured (at about 00:25 LT); this

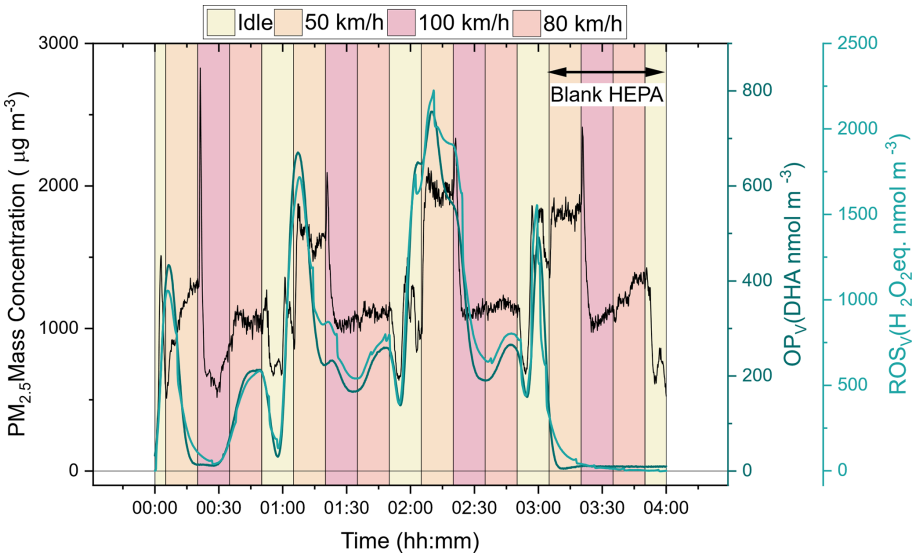

Figure 2. OP_V and ROS_V measurement of secondary car emissions after an equivalent of 2.1 d of ageing during four driving cycles as well as the particle mass measured by an ELPI. OP_V and ROS_V are given in nanomoles of DHA per cubic metre and nanomoles of H_2O_2 equivalent per cubic metre, respectively. The last hour of measurements after 3 h was used for a HEPA blank, removing all particles from the sample flow.

could have been due to the strong acceleration of the engine, similarly to the transition from idle to 50 km h^{-1}, causing non-ideal combustion conditions.

The ROS_M concentrations of the two photochemical ageing conditions are shown in Fig. 4. Overall, the ROS behaviour was similar to the OP_M results across all driving conditions: 40 % higher ROS_M values were observed during the transition from idle to 50 km h^{-1} compared with the concentrations measured during 100 and 80 km h^{-1} periods, and the same slight and a transient increase of approximately 30 % was noted at the beginning of the 100 km h^{-1} (00:25 LT) condition. Unlike the OP_M, the ROS_M signal decreased with ageing and was 30 %–70 % higher during short-term ageing (Fig. 4a) compared with medium-term ageing (Fig. 4b) across all driving conditions. A possible explanation for this decrease in ROSs with increasing ageing time could be the photolytic decomposition of peroxides over time. Other studies using an atmospheric simulation chamber have also observed a decrease in ROS activity with longer photochemical ages (several hours to days) for two-stroke scooter engine emissions as well as biogenic SOA (Epstein et al., 2014; Platt et al., 2014).

The OP and ROS activity values during cold starts at the beginning of an experiment were not distinguishable from the following driving cycles (warm start) during a 4 h experiment. Because the cold start is very short (5 min) and, thus, within the time resolution of both the OOPAAI and OPROSI instruments, the difference from cold start could not be resolved; therefore, it was not analysed separately.

3.2 OP and ROS concentrations from residential wood combustion (RWC) particles

For the RWC experiments, both primary emissions and two ageing conditions were investigated. In Fig. 5, OP_V and ROS_V measurements are shown as well as the particle mass measured by an ELPI during a 4 h experiment with RWC aged for an equivalent of up to 3.3 d. Light- and darker-blue background colours indicate the addition of a new wood batch (see Sect. 2). The last batch was left to burn for an additional 30 min as the ember phase (yellow background in Fig. 5).

Both instruments observed an increase and subsequent decrease in OP_V and ROS_V, respectively, with each batch. OP_V and ROS_V reached peak values in the first half of a 35 min long batch that were approximately a factor of 10 higher compared with values at the end of a batch. This again demonstrates how both online instruments are capable of capturing fast-changing emission characteristics. After six batches of wood added to the stove, the ember phase started, characterised by low emissions of OP_V and ROS_V as well as particles. Compared with the car experiments, the RWC results showed a higher batch-to-batch variability, which was observed by both instruments as well as the particle mass concentration, as also reported in previous RWC studies (Heringa et al., 2012; Vicente et al., 2015).

In contrast to the car emissions, where no primary particles were emitted due to the GPF, both instruments responded to the primary RWC emissions. The OOPAAI observed an OP_V signal for primary emission that was up to 3 times lower than during the aged experiments (Fig. S6), as can be expected

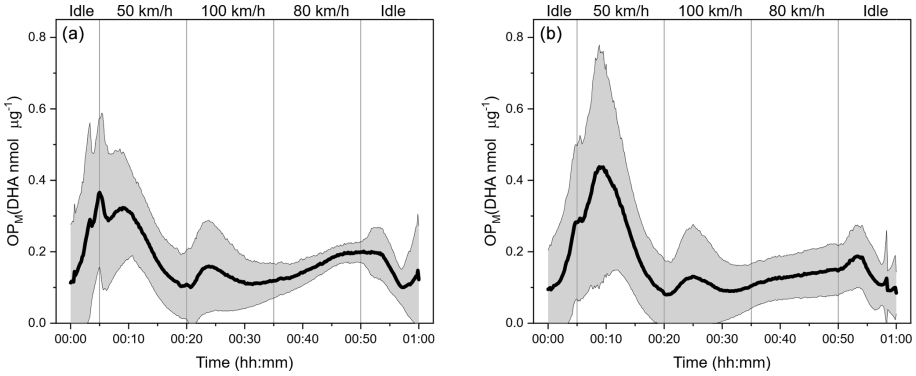

Figure 3. OP_M concentrations after 2.1 d **(a)** and 5.1 d **(b)** of photochemical ageing of car emissions. The average of 15 driving cycles is represented in 1 cycle (black line). The error band (grey shading) shown is the standard deviation of the 15 driving cycles.

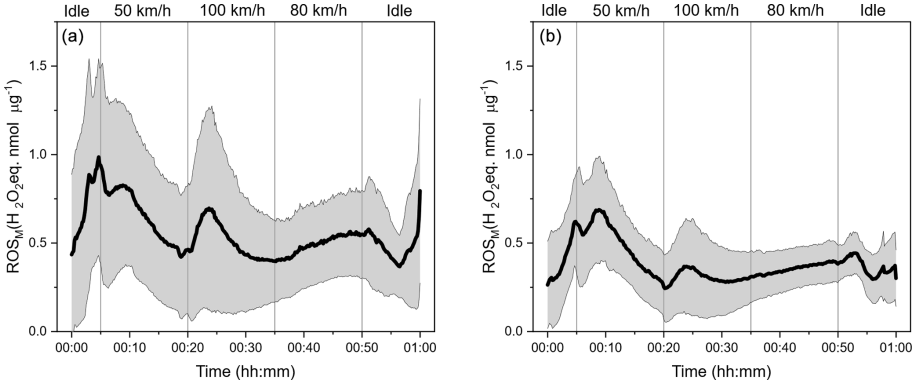

Figure 4. ROS_M concentration of 2.1 d **(a)** and 5.1 d **(b)** in aged car emissions. The average is 15 driving cycles for short-term ageing, whereas medium-term ageing is represented in 1 cycle (black line). The error band (grey shading) shown is the standard deviation of the 15 driving cycles.

because ROSs are predominantly formed through oxidation processes.

In contrast, the OPROSI showed a different response to primary RWC particles, with negative ROS values (Fig. S5), which might be a measurement artefact of the large fraction of insoluble primary PM (e.g. soot). Due to the high PM and, specifically, soot concentrations during these emission measurements, particles accumulated inside the instruments and potentially interacted with and deactivated the assay, causing the ROS signal to fall below blank values. The hydrophobic and large surface area of the soot particles could adsorb and inactivate reagents of the assay (e.g. HRP), causing an apparent lower ROS concentration compared with the blank. Enzymes are known to change their activity due to absorption onto a high-surface-area substrate (Khan, 2021) To test this hypothesis in a qualitative way, activated charcoal was mixed with the ROS assay as a proxy for soot, as it also has a high hydrophobic surface area. Figure S6 shows a clear decrease in the ROS signal with higher concentrations of charcoal, which is a fundamental limitation of the DCFH assay at very high insoluble particle concentrations. Organic components in the primary particles, e.g. antioxidant compounds frequently found in wood smoke such as phenols, could also cause a signal decrease by reacting with HRP (Kjällstrand and Petersson, 2001) The negative ROS peaks were less than 10 % of the positive signals for the aged exhaust; thus, any uncertainties of aged ROS values related to the very high soot or antioxidant conditions are likely in the same range.

In Fig. 6, the OP_M of the primary aerosol and the two ageing conditions are shown with the standard deviation from 16–21 repeat measurements. Two different ageing conditions with 1.4 ± 0.2 d (short) and 3.3 ± 0.4 d (medium) were investigated. The ember phase is not considered in these figures, as it did not show any detectable OP or ROS activity (data not shown). The primary aerosol (Fig. 6a) resulted in low (between 0 and 2 DHA nmol µg^{-1}) and stable OP_M values in the same range as the car emissions for the majority of a batch. Near the end, when the wood was almost burned up and when no flames were visible anymore in some cases, OP_M increased sharply by up to a factor of 6 compared with the rest of the batch. A continuous increase was observed during the short-term ageing condition, with peak values being reached in the last 10 min of a batch (Fig. 6b). For the short-term ageing condition,

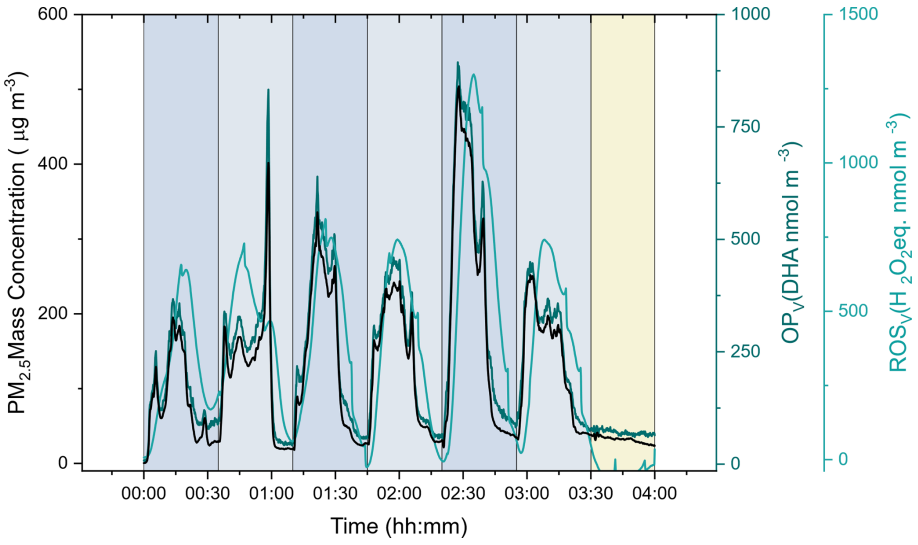

Figure 5. OP_V (dark-green) and ROS_V (light-green) measurement of one secondary RWC emission experiment as well as the particle mass (left axis, black line) measured by an ELPI. The blue boxes mark the different batches of wood added to the oven, whereas the yellow box is the ember phase.

the average OP_M values remained comparable to the primary aerosol during the same time period within a large batch-to-batch variability (5.19 ± 9.48 nmol DHA μg^{-1} vs. 6.48 ± 8.30 nmol DHA μg^{-1}, respectively). For the medium-term ageing condition, the large increase in OP_M at the end of a batch (as seen for primary emissions and short-term ageing) was no longer observed, while OP_M concentrations still increased continuously during the course of a batch, similar to short-term ageing conditions (Fig. 6B). This resulted in an overall lower OP_M with medium-term ageing.

The reduction in OP_M from short-term to medium-term ageing could be due to chemical changes in PM components caused by prolonged oxidation reactions. For example, the oxidation of polycyclic aromatic hydrocarbons (PAHs) in the atmosphere, formed during wood combustion, can lead to the formation of quinone-type products (Walgraeve et al., 2010), which are known to produce ROSs in an aqueous solution and, therefore, would also contribute to OP in the OOPAAI (Charrier and Anastasio, 2012; Li et al., 2003; Njus et al., 2023).

However, continued oxidation during medium-term ageing may result in further oxidation of such OP-active quinones into inactive compounds, which would result in a lower OP activity. This effect has been observed for markers of biomass-burning SOA before via the breakdown of aromatic rings (Fang et al., 2024). Wong et al. (2019) observed an overall decrease in OP in aged laboratory-generated biomass-burning aerosol after a short initial increase, similar to our OP measurements with ascorbic acid. This overall decrease with higher ageing could also partially be explained by the decrease in quinone concentrations in wood smoke observed with higher ages (Jiang and Jang, 2018). Moreover, for certain SOA types from the gaseous precursors β-pinene and naphthalene, it was observed (using the DCFH assay) that more ageing does not induce a higher OP (Offer et al., 2022). Figure 6 shows the ROS_M values for the two ageing conditions. For the primary RWC aerosol, ROS signals could not be determined, as discussed above. Similar to OP_M, the highest ROS_M values were observed in later parts of a batch for both ageing conditions. However, this trend was more pronounced during the medium-term ageing experiments, in contrast to OP_M. ROS_M was 3 times lower during short-term ageing (Fig. 7a) compared with the medium-term ageing results (Fig. 7b). More oxidised aerosol is generally associated with the more oxygenated fraction of PM such as peroxides, to which the DCFH assay is especially sensitive (Fang et al., 2024; Li et al., 2021; Nordin et al., 2015; Wang et al., 2023; Zhang et al., 2022). This is in agreement with the ageing of wood smoke in an atmospheric simulation chamber, where ageing by OH also lead to an increase in ROS activity (Wang et al., 2023). Furthermore, Zhang et al. (2022) measured an increase in ROSs with higher ageing times for two simple SOA systems using β-pinene and naphthalene as precursors (Zhang et al., 2022).

3.3 Comparison of OP_M and ROS_M and emission factors of car exhaust and RWC

Table 1 summarises the OP_M and ROS_M values that we observed, covering a realistic range of atmospheric oxidative processing times up to 5 d. The OP_M and ROS_M activity values measured during this study were highly dynamic, changing up to 2 orders of magnitude within minutes, and are comparable to other lab studies characterising pure SOA sys-

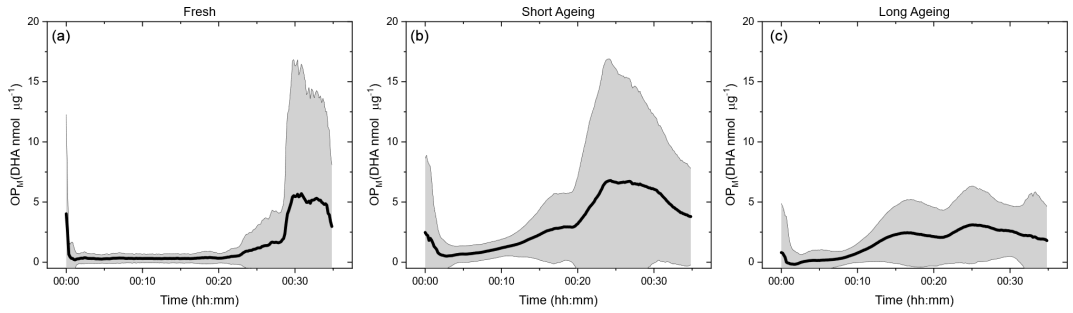

Figure 6. Average OP_M of 0 d (fresh, 21 batches; **a**), 1.4 ± 0.2 d (short, 16 batches; **b**), and 3.3 ± 0.4 d (medium, 17 batches; **c**) RWC emissions (black line). The error shown is the standard deviation of the averaged batches (grey shading).

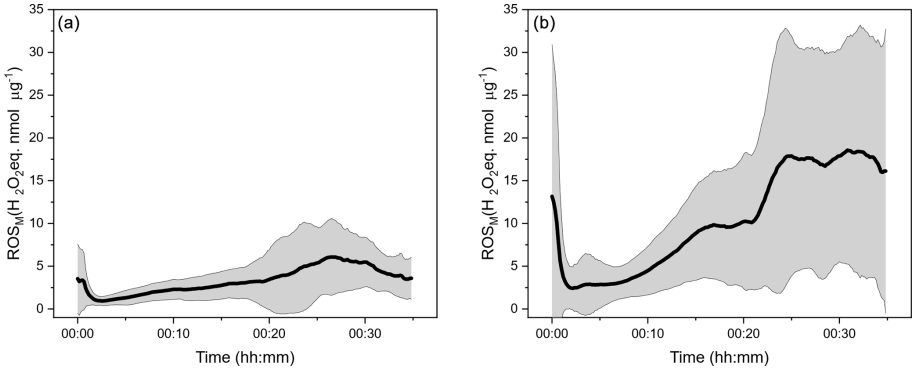

Figure 7. Average ROS_M concentrations for 1.4 ± 0.2 d (short, 16 batches; **a**) and 3.3 ± 0.4 d (medium, 17 batches; **b**) RWC emissions (black line). The standard deviation of the different measurements is plotted as an error band (grey shading).

Table 1. Overview of the measured OP_M and ROS_M values, illustrating the large range observed within a cycle (car) or batch (RWC) as a result of the high-temporal-resolution online measurements. To determine the atmospheric age (in days) for the RWC measurements, the average and standard deviation of five ageing condition measurements are given, whereas only one measurement per age was conducted for the car exhaust.

Source	Age (days)	OP_M (nmol DHA µg^{-1})	ROS_M (nmol H_2O_2 eq. µg^{-1})
Car	0.0	NA	NA
	2.1	0.1–0.4	0.4–1.0
	5.1	0.1–0.4	0.2–0.7
RWC	0.0	0.2-5.7	NA
	1.4 ± 0.2	0.5–6.8	0.9–6.1
	3.3 ± 0.4	0.0–3.1	2.4–18.6

NA: not available.

tems conducted with similar online instruments (Campbell et al., 2023; Zhang et al., 2022).

A comparison of primary particles is not possible, as the car has a GPF and, therefore, produces almost no primary particle emissions, in contrast to the stove that produces more primary particles. This means that the combined effects of primary and secondary aerosols on the OP and ROS activity were observed during the stove experiments, whereas only secondary car particles were measured. The lack of primary particles could partially be responsible for the higher (up to 1 order of magnitude) OP_M and ROS_M values from the wood stove. The large difference in OP_M and ROS_M between car and RWC emissions could also be explained by the difference in the composition of the secondary particles. A compositional difference is the metal content of the two aerosol types. Wood smoke is known to contain a wide range of redox-active metals, including zinc, iron, and copper (Erlandsson et al., 2020; Gonçalves et al., 2010; Uski et al., 2015) The total metal concentrations can reach up to 2.5 wt % of $PM_{2.5}$ depending on the wood type and combustion appliance, whereas car exhaust treated with a particulate filter only contains very low concentration of metallic primary particles and consists mostly of secondary aerosol (Alves et al., 2011). The presence of transition metals has been shown to have an influence on the OP and ROS activity of SOA. Campbell et al. (2023) observed synergistic effects leading to higher OP_M when biogenic SOA and metals were combined. In addition, differences in the SOA composition from these two sources also likely contribute to the observed differences in OP_M and ROS_M.

Emission factors are calculated and used to estimate the quantity of pollutants released into the atmosphere from vari-

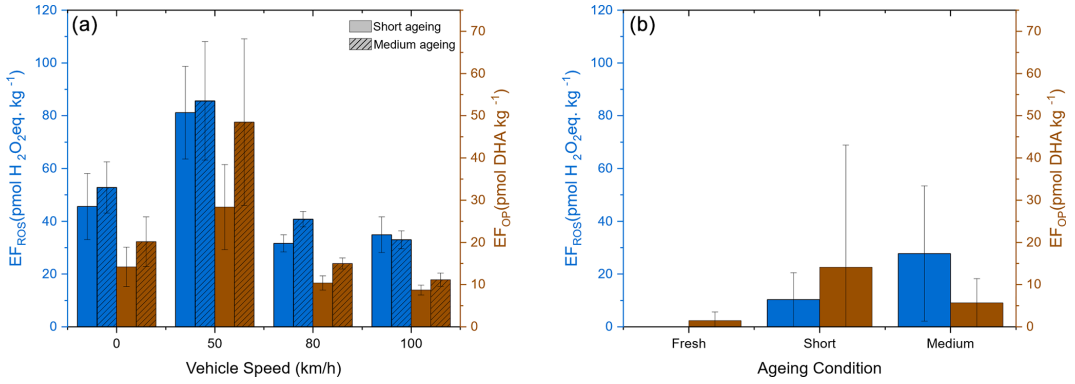

Figure 8. Emission factors for car emissions **(a)** and RWC **(b)**. The blue bars represent EF_{ROS}, whereas EF_{OP} is shown in brown. The striped bars represent the medium-term ageing condition, whereas the plain bars show short-term ageing. The error bars shown represent the standard deviation of the averaged values and indicate the variability in the measurements.

ous sources, thereby helping to assess environmental impacts and guide regulatory compliance and mitigation efforts. To the best of our knowledge, emission factors of OP and ROSs have never been reported in the literature before. Figure 8a shows EF_{OP} and EF_{ROS} for different driving speeds and both ageing conditions in picomoles of DHA per kilogram of fuel and picomoles of H_2O_2 equivalent per kilogram of fuel, respectively. Similar to the PM-mass-normalised OP and ROS results, the 50 km h^{-1} condition resulted in the highest EF values. Medium-term ageing led to an overall increase in EF_{OP} and EF_{ROS}. The smallest change was observed for a speed of 100 km h^{-1}. Figure 8b shows emission factors for RWC for fresh emissions as well as short-term and medium-term ageing. Opposite effects of ageing on the two assays are visible, similar to trends in the mass-normalised OP_M and ROS_M data (Figs. 6, 7): an increase in ageing leads to a reduction in EF_{OP} but to an increase in EF_{ROS}. No clear trend in EF_{ROS} between the two ageing conditions (blue denotes short-term ageing and blue stripes denote medium-term ageing for the car and short-term and medium-term for RWC) was detected. EF_{ROS} and EF_{OP} for petrol car emissions are up to 8 times higher than RWC values, which is the opposite compared with the mass-normalised OP_M and ROS_M concentrations. This can be explained, in part, by the very different units used for normalising OP_M and EF. For OP_M, the mass of emitted particles is used to normalise OP values, whereas the mass of burnt fuel is used for EF. EF_{OP} and EF_{ROS} could be a useful metric to compare the OP and ROSs per kilogram of fuel to assess the relative toxicity of emissions from different combustion sources.

4 Conclusion

The OP and ROS concentrations of aged and fresh emissions from a petrol car and a wood burning stove were characterised with two online, high-temporal-resolution instruments. On average, the RWC emissions had OP_M and ROS_M values that were up to 10 times higher compared with the car emissions. Atmospheric ageing affects the OP_M and ROS_M content in the particle emissions of these two sources differently: for RWC, an increased OP_M was observed with short-term ageing compared with the fresh emissions and medium-term ageing; however, for car exhaust, longer ageing leads to a slightly higher OP_M.

In contrast, the ROS_M content decreased with longer ageing for the car emissions. For the RWC emissions, the opposite was observed: the ROS_M concentration increased with longer ageing.

The highly dynamic changes in OP and ROS activity within one car driving cycle or wood batch and the large batch-to-batch variability in values (often on timescales of a few minutes) would not be detectable with traditional offline methods.

Our data indicate that the contribution of RWC emissions per microgram of particle emissions towards PM toxicity is significantly larger than that from petrol car emissions. However, this is also due to the implementation of GPFs, which prevent most primary car emissions.

Biomass burning is the main emission source from the residential sector and can contribute more than 50 % of anthropogenic $PM_{2.5}$ emissions in some parts of Europe (Zauli-Sajani et al., 2024) The $PM_{2.5}$ mass contribution of biomass burning was shown to be as high as that from traffic exhaust, even at traffic sites, in five European cities (Saraga et al., 2021) Combined with the high OP and ROS activity of RWC emissions, the potential detrimental effects on human health should be considered in air quality efforts. In addition, the SOA particle formation potential of car emissions with high OP and ROS activities can be observed, even if there are almost no primary particle emissions (as demonstrated in this study). Overall, the results presented here show the importance of measuring the OP and ROSs with a high temporal resolution to capture their dynamic nature and to consider the different atmospheric ageing times of these potential PM toxicity markers.

Data availability. All data can be accessed from the corresponding author upon request.

Supplement. The supplement related to this article is available online at https://doi.org/10.5194/ar-3-205-2025-supplement.

Author contributions. BU and AB: investigation, methodology, formal analysis, visualisation, and writing – original draft preparation; AP, AM, C-MM, MI, PYP, MiK, ZF, PM, MS, and JL: investigation; SJC, HC, and OS: conceptualisation and writing – reviewing and editing; TH, YR, and RZ: resources; and MaK: conceptualisation, supervision, resources, and writing – reviewing and editing.

Competing interests. The contact author has declared that none of the authors has any competing interests.

Disclaimer. Publisher's note: Copernicus Publications remains neutral with regard to jurisdictional claims made in the text, published maps, institutional affiliations, or any other geographical representation in this paper. While Copernicus Publications makes every effort to include appropriate place names, the final responsibility lies with the authors.

Acknowledgements. The authors are grateful to the Swiss National Science Foundation (SNF; grant no. 192192), the Helmholtz International Laboratory aeroHEALTH (InterLabs-0005; https://aerohealth.eu, last access: 31 March 2025), and the ULTRHAS Horizon Europe project (grant no. 955390) for supporting this work. We also wish to thank the members of the aeroHEALTH consortium that contributed to the measurement campaign.

Financial support. This research has been supported by the Schweizerischer Nationalfonds zur Förderung der Wissenschaftlichen Forschung (grant no. 192192) and the EU Horizon 2020 (grant no. 955390).

Review statement. This paper was edited by Daniele Contini and reviewed by two anonymous referees.

References

Alves, C., Gonçalves, C., Fernandes, A. P., Tarelho, L., and Pio, C.: Fireplace and woodstove fine particle emissions from combustion of western Mediterranean wood types, Atmos. Res., 101, 692–700, https://doi.org/10.1016/J.ATMOSRES.2011.04.015, 2011.

Atkinson, R. W., Mills, I. C., Walton, H. A., and Anderson, H. R.: Fine particle components and health–a systematic review and meta-analysis of epidemiological time series studies of daily mortality and hospital admissions, J. Expo. Sci. Env. Epid., 25, 208–214, https://doi.org/10.1038/jes.2014.63, 2015.

Bates, J. T., Fang, T., Verma, V., Zeng, L., Weber, R. J., Tolbert, P. E., Abrams, J. Y., Sarnat, S. E., Klein, M., Mulholland, J. A., and Russell, A. G.: Review of Acellular Assays of Ambient Particulate Matter Oxidative Potential: Methods and Relationships with Composition, Sources, and Health Effects, Environ. Sci. Technol., 53, 4003–4019, https://doi.org/10.1021/acs.est.8b03430, 2019.

Baulig, A., Garlatti, M., Bonvallot, V., Marchand, A., Barouki, R., Marano, F., and Baeza-Squiban, A.: Involvement of reactive oxygen species in the metabolic pathways triggered by diesel exhaust particles in human airway epithelial cells, Am. J. Physiol.-Lung C., 285, L671–L679 https://doi.org/10.1152/ajplung.00419.2002, 2003.

Brunekreef, B. and Holgate, S. T.: Air pollution and health, The Lancet, 360, 1233–1242, https://doi.org/10.1016/S0140-6736(02)11274-8, 2002.

Campbell, S. J., Stevanovic, S., Miljevic, B., Bottle, S. E., Ristovski, Z., and Kalberer, M.: Quantification of Particle-Bound Organic Radicals in Secondary Organic Aerosol, Environ. Sci. Technol., 53, 6729–6737, https://doi.org/10.1021/acs.est.9b00825, 2019.

Campbell, S. J., Utinger, B., Barth, A., Paulson, S. E., and Kalberer, M.: Iron and Copper Alter the Oxidative Potential of Secondary Organic Aerosol: Insights from Online Measurements and Model Development, Environ. Sci. Technol., 57, 13546–13558, https://doi.org/10.1021/ACS.EST.3C01975, 2023.

Campbell, S. J., Barth, A., Chen, G. I., Tremper, A. H., Priestman, M., Ek, D., Gu, S., Kelly, F. J., Kalberer, M., and Green, D. C.: High time resolution quantification of $PM_{2.5}$ oxidative potential at a Central London roadside supersite, Environ. Int., 193, 109102, https://doi.org/10.1016/j.envint.2024.109102, 2024.

Charrier, J. G. and Anastasio, C.: On dithiothreitol (DTT) as a measure of oxidative potential for ambient particles: evidence for the importance of soluble transition metals, Atmos. Chem. Phys., 12, 9321–9333, https://doi.org/10.5194/acp-12-9321-2012, 2012.

Daellenbach, K. R., Uzu, G., Jiang, J., Cassagnes, L.-E., Leni, Z., Vlachou, A., Stefenelli, G., Canonaco, F., Weber, S., Segers, A., Kuenen, J. J. P., Schaap, M., Favez, O., Albinet, A., Aksoyoglu, S., Dommen, J., Baltensperger, U., Geiser, M., El Haddad, I., Jaffrezo, J.-L., and Prévôt, A. S. H.: Sources of particulate-matter air pollution and its oxidative potential in Europe, Nature, 587, 414–419, https://doi.org/10.1038/s41586-020-2902-8, 2020.

Denier van der Gon, H. A. C., Bergström, R., Fountoukis, C., Johansson, C., Pandis, S. N., Simpson, D., and Visschedijk, A. J. H.: Particulate emissions from residential wood combustion in Europe – revised estimates and an evaluation, Atmos. Chem. Phys., 15, 6503–6519, https://doi.org/10.5194/acp-15-6503-2015, 2015.

Donaldson, K., Stone, V., Seaton, A., and MacNee, W.: Ambient particle inhalation and the cardiovascular system: Potential mechanisms, Environ. Health Persp., 109, 523–527, https://doi.org/10.1289/ehp.01109s4523, 2001.

Epstein, S. A., Blair, S. L., and Nizkorodov, S. A.: Direct Photolysis of α-Pinene Ozonolysis Secondary Organic Aerosol: Effect on Particle Mass and Peroxide Content, Environ. Sci. Technol., 48, 11251–11258, https://doi.org/10.1021/es502350u, 2014.

Erlandsson, L., Lindgren, R., Nääv, Å., Krais, A. M., Strandberg, B., Lundh, T., Boman, C., Isaxon, C., Hansson, S.

R., and Malmqvist, E.: Exposure to wood smoke particles leads to inflammation, disrupted proliferation and damage to cellular structures in a human first trimester trophoblast cell line, Environ. Pollut., 264, 114790, https://doi.org/10.1016/J.ENVPOL.2020.114790, 2020.

Council of the European Union: Directive (EU) 2024/2881 of the European Parliament and of the Council of 23 October 2024 on ambient air quality and cleaner air for Europe (recast), Document 32024L2881, PE/88/2024/REV/1 OJ L, 2024/2881, http://data.europa.eu/eli/dir/2024/2881/oj (last access: 31 March 2025), 2024.

Fang, Z., Lai, A., Dongmei Cai, Chunlin Li, Carmieli, R., Chen, J., Wang, X., and Rudich, Y.: Secondary Organic Aerosol Generated from Biomass Burning Emitted Phenolic Compounds: Oxidative Potential, Reactive Oxygen Species, and Cytotoxicity, Environ. Sci. Technol., 58, 8194–8206, https://doi.org/10.1021/acs.est.3c09903, 2024.

Gao, J., Chen, H., Liu, Y., Laurikko, J., Li, Y., Li, T., and Tu, R.: Comparison of NO_x and PN emissions between Euro 6 petrol and diesel passenger cars under real-world driving conditions, Sci. Total Environ., 801, 149789, https://doi.org/10.1016/j.scitotenv.2021.149789, 2021.

Gonçalves, C., Alves, C., Evtyugina, M., Mirante, F., Pio, C., Caseiro, A., Schmidl, C., Bauer, H., and Carvalho, F.: Characterisation of PM_{10} emissions from woodstove combustion of common woods grown in Portugal, Atmos. Environ., 44, 4474–4480, https://doi.org/10.1016/j.atmosenv.2010.07.026, 2010.

Guascito, M. R., Lionetto, M. G., Mazzotta, F., Conte, M., Giordano, M. E., Caricato, R., De Bartolomeo, A. R., Dinoi, A., Cesari, D., Merico, E., Mazzotta, L., and Contini, D.: Characterisation of the correlations between oxidative potential and in vitro biological effects of PM_{10} at three sites in the central Mediterranean, J. Hazard. Mater., 448, 130872, https://doi.org/10.1016/j.jhazmat.2023.130872, 2023.

Hart, J. E., Liao, X., Hong, B., Puett, R. C., Yanosky, J. D., Suh, H., Kioumourtzoglou, M. A., Spiegelman, D., and Laden, F.: The association of long-term exposure to $PM_{2.5}$ on all-cause mortality in the Nurses' Health Study and the impact of measurement-error correction, Environmental Health, 14, 38, https://doi.org/10.1186/s12940-015-0027-6, 2015.

Hartikainen, A. H., Ihalainen, M., Yli-Pirilä, P., Hao, L., Kortelainen, M., Pieber, S. M., and Sippula, O.: Photochemical transformation and secondary aerosol formation potential of Euro6 gasoline and diesel passenger car exhaust emissions, J. Aerosol Sci., 171, 106159, https://doi.org/10.1016/j.jaerosci.2023.106159, 2023.

Heo, J., Schauer, J. J., Yi, O., Paek, D., Kim, H., and Yi, S.-M.: Fine Particle Air Pollution and Mortality: Importance of Specific Sources and Chemical Species, Epidemiology, 25, 379–388, https://doi.org/10.1097/EDE.0000000000000044, 2014.

Heringa, M. F., DeCarlo, P. F., Chirico, R., Lauber, A., Doberer, A., Good, J., Nussbaumer, T., Keller, A., Burtscher, H., Richard, A., Miljevic, B., Prevot, A. S. H., and Baltensperger, U.: Time-Resolved Characterization of Primary Emissions from Residential Wood Combustion Appliances, Environ. Sci. Technol., 46, 11418–11425, https://doi.org/10.1021/es301654w, 2012.

Ihalainen, M., Tiitta, P., Czech, H., Yli-Pirilä, P., Hartikainen, A., Kortelainen, M., Tissari, J., Stengel, B., Sklorz, M., Suhonen, H., Lamberg, H., Leskinen, A., Kiendler-Scharr, A., Harndorf, H., Zimmermann, R., Jokiniemi, J., and Sippula, O.: A novel high-volume Photochemical Emission Aging flow tube Reactor (PEAR), Aerosol Sci. Tech., 53, 276–294, https://doi.org/10.1080/02786826.2018.1559918, 2019.

Ihantola, T., Hirvonen, M.-R., Ihalainen, M., Hakkarainen, H., Sippula, O., Tissari, J., Bauer, S., Di Bucchianico, S., Rastak, N., Hartikainen, A., Leskinen, J., Yli-Pirilä, P., Martikainen, M.-V., Miettinen, M., Suhonen, H., Rönkkö, T. J., Kortelainen, M., Lamberg, H., Czech, H., Martens, P., Orasche, J., Michalke, B., Yildirim, A. Ö., Jokiniemi, J., Zimmermann, R., and Jalava, P. I.: Genotoxic and inflammatory effects of spruce and brown coal briquettes combustion aerosols on lung cells at the air-liquid interface, Sci. Total Environ., 806, 150489, https://doi.org/10.1016/j.scitotenv.2021.150489, 2022.

Jiang, H. and Jang, M.: Dynamic Oxidative Potential of Atmospheric Organic Aerosol under Ambient Sunlight, Environ. Sci. Technol., 52, 7496–7504, https://doi.org/10.1021/acs.est.8b00148, 2018.

Kelly, F. J.: Oxidative stress: its role in air pollution and adverse health effects, Occup. Environ. Med., 60, 612–616, https://doi.org/10.1136/oem.60.8.612, 2003.

Kelly, F. J. and Fussell, J. C.: Size, source and chemical composition as determinants of toxicity attributable to ambient particulate matter, Atmos. Environ., 60, 504–526, https://doi.org/10.1016/j.atmosenv.2012.06.039, 2012.

Khan, M. R.: Immobilized enzymes: a comprehensive review, Bulletin of the National Research Centre, 45, 207, https://doi.org/10.1186/s42269-021-00649-0, 2021.

Kjällstrand, J. and Petersson, G.: Phenolic antioxidants in wood smoke, Sci. Total Environ., 277, 69–75, https://doi.org/10.1016/S0048-9697(00)00863-9, 2001.

Künzi, L., Krapf, M., Daher, N., Dommen, J., Jeannet, N., Schneider, S., Platt, S., Slowik, J. G., Baumlin, N., Salathe, M., Prévôt, A. S. H., Kalberer, M., Strähl, C., Dümbgen, L., Sioutas, C., Baltensperger, U., and Geiser, M.: Toxicity of aged gasoline exhaust particles to normal and diseased airway epithelia, Scientific Reports, 5, 1–10, https://doi.org/10.1038/srep11801, 2015.

Laden, F., Schwartz, J., Speizer, F. E., and Dockery, D. W.: Reduction in fine particulate air pollution and mortality: Extended follow-up of the Harvard Six Cities Study, Am. J. Resp. Crit. Care, 173, 667–672, https://doi.org/10.1164/rccm.200503-443OC, 2006.

Lepeule, J., Laden, F., Dockery, D., and Schwartz, J.: Chronic exposure to fine particles and mortality: An extended follow-up of the Harvard six cities study from 1974 to 2009, Environmental Health Perspectives, 120, 965–970, https://doi.org/10.1289/ehp.1104660, 2012.

Leskinen, J., Hartikainen, A., Väätäinen, S., Ihalainen, M., Virkkula, A., Mesceriakovas, A., Tiitta, P., Miettinen, M., Lamberg, H., Czech, H., Yli-Pirilä, P., Tissari, J., Jakobi, G., Zimmermann, R., and Sippula, O.: Photochemical Aging Induces Changes in the Effective Densities, Morphologies, and Optical Properties of Combustion Aerosol Particles, Environ. Sci. Technol., 57, 5137–5148, https://doi.org/10.1021/acs.est.2c04151, 2023.

Li, J., Li, J., Wang, G., Ho, K. F., Dai, W., Zhang, T., Wang, Q., Wu, C., Li, L., Li, L., and Zhang, Q.: Effects of atmospheric aging processes on in vitro induced oxidative stress and chemical composition of biomass burning aerosols, J. Hazard. Mater.,

401, 123750, https://doi.org/10.1016/J.JHAZMAT.2020.123750, 2021.

Li, N., Hao, M., Phalen, R. F., Hinds, W. C., and Nel, A. E.: Particulate air pollutants and asthma: A paradigm for the role of oxidative stress in PM-induced adverse health effects, Clinical Immunology, 109, 250–265, https://doi.org/10.1016/j.clim.2003.08.006, 2003.

Martens, P., Czech, H., Tissari, J., Ihalainen, M., Suhonen, H., Sklorz, M., Jokiniemi, J., Sippula, O., and Zimmermann, R.: Emissions of Gases and Volatile Organic Compounds from Residential Heating: A Comparison of Brown Coal Briquettes and Logwood Combustion, Energ. Fuel., 35, 14010–14022, https://doi.org/10.1021/acs.energyfuels.1c01667, 2021.

Mukherjee, A., Hartikainen, A., Joutsensaari, J., Basnet, S., Mesceriakovas, A., Ihalainen, M., Yli-Pirilä, P., Leskinen, J., Somero, M., Louhisalmi, J., Fang, Z., Kalberer, M., Rudich, Y., Tissari, J., Czech, H., Zimmermann, R., and Sippula, O.: Black carbon and particle lung-deposited surface area in residential wood combustion emissions: Effects of an electrostatic precipitator and photochemical aging, Sci. Total Environ., 952, 175840, https://doi.org/10.1016/j.scitotenv.2024.175840, 2024.

Njus, D., Asmaro, K., Li, G., and Palomino, E.: Redox cycling of quinones reduced by ascorbic acid, Chem.-Biol. Interact., 373, 110397, https://doi.org/10.1016/J.CBI.2023.110397, 2023.

Nordin, E. Z., Uski, O., Nyström, R., Jalava, P., Eriksson, A. C., Genberg, J., Roldin, P., Bergvall, C., Westerholm, R., Jokiniemi, J., Pagels, J. H., Boman, C., and Hirvonen, M. R.: Influence of ozone initiated processing on the toxicity of aerosol particles from small scale wood combustion, Atmos. Environ., 102, 282–289, https://doi.org/10.1016/j.atmosenv.2014.11.068, 2015.

Offer, S., Hartner, E., Di Bucchianico, S., Bisig, C., Bauer, S., Pantzke, J., Zimmermann, E. J., Cao, X., Binder, S., Kuhn, E., Huber, A., Jeong, S., Käfer, U., Martens, P., Mesceriakovas, A., Bendl, J., Brejcha, R., Buchholz, A., Gat, D., Hohaus, T., Rastak, N., Jakobi, G., Kalberer, M., Kanashova, T., Hu, Y., Ogris, C., Marsico, A., Theis, F., Pardo, M., Gröger, T., Oeder, S., Orasche, J., Paul, A., Ziehm, T., Zhang, Z.-H. H., Adam, T., Sippula, O., Sklorz, M., Schnelle-Kreis, J., Czech, H., Kiendler-Scharr, A., Rudich, Y., and Zimmermann, R.: Effect of Atmospheric Aging on Soot Particle Toxicity in Lung Cell Models at the Air–Liquid Interface: Differential Toxicological Impacts of Biogenic and Anthropogenic Secondary Organic Aerosols (SOAs), Environ. Health Persp., 130, 1–19, https://doi.org/10.1289/EHP9413, 2022.

Orru, H., Olstrup, H., Kukkonen, J., López-Aparicio, S., Segersson, D., Geels, C., Tamm, T., Riikonen, K., Maragkidou, A., Sigsgaard, T., Brandt, J., Grythe, H., and Forsberg, B.: Health impacts of $PM_{2.5}$ originating from residential wood combustion in four nordic cities, BMC Public Health, 22, 1–13, https://doi.org/10.1186/s12889-022-13622-x, 2022.

Øvrevik, J., Refsnes, M., Låg, M., Holme, J. A., and Schwarze, P. E.: Activation of Proinflammatory Responses in Cells of the Airway Mucosa by Particulate Matter: Oxidant- and Non-Oxidant-Mediated Triggering Mechanisms, Biomolecules, 5, 1399–1440, https://doi.org/10.3390/biom5031399, 2015.

Paul, A., Fang, Z., Martens, P., Mukherjee, A., Jakobi, G., Ihalainen, M., Kortelainen, M., Somero, M., Yli-Pirilä, P., Hohaus, T., Czech, H., Kalberer, M., Sippula, O., Rudich, Y., Zimmermann, R., and Kiendler-Scharr, A.: Formation of secondary aerosol from emissions of a Euro 6d-compliant gasoline vehicle with particle filter, Environ. Sci.: Atmos., 4, 802–812, https://doi.org/10.1039/D3EA00165B, 2024.

Pizzino, G., Irrera, N., Cucinotta, M., Pallio, G., Mannino, F., Arcoraci, V., Squadrito, F., Altavilla, D., and Bitto, A.: Oxidative Stress: Harms and Benefits for Human Health, Oxid. Med. Cell. Longev., 8416763, 13 pp., https://doi.org/10.1155/2017/8416763, 2017.

Platt, S. M., Haddad, I. El., Pieber, S. M., Huang, R.-J., Zardini, A. A., Clairotte, M., Suarez-Bertoa, R., Barmet, P., Pfaffenberger, L., Wolf, R., Slowik, J. G., Fuller, S. J., Kalberer, M., Chirico, R., Dommen, J., Astorga, C., Zimmermann, R., Marchand, N., Hellebust, S., Temime-Roussel, B., Baltensperger, U., and Prévôt, A. S. H.: Two-stroke scooters are a dominant source of air pollution in many cities, Nat. Commun., 5, 3749, https://doi.org/10.1038/ncomms4749, 2014.

Platt, S. M., El Haddad, I., Pieber, S. M., Zardini, A. A., Suarez-Bertoa, R., Clairotte, M., Daellenbach, K. R., Huang, R.-J., Slowik, J. G., Hellebust, S., Temime-Roussel, B., Marchand, N., De Gouw, J., Jimenez, J. L., Hayes, P. L., Robinson, A. L., Baltensperger, U., Astorga, C., and Prévôt, A. S. H.: Gasoline cars produce more carbonaceous particulate matter than modern filter-equipped diesel cars, Scientific Reports, 7, 4926, https://doi.org/10.1038/s41598-017-03714-9, 2017.

Prahalad, A. K., Inmon, J., Dailey, L. A., Madden, M. C., Ghio, A. J., and Gallagher, J. E.: Air pollution particles mediated oxidative DNA base damage in a cell free system and in human airway epithelial cells in relation to particulate metal content and bioreactivity, Chem. Res. Toxicol., 14, 879–887, https://doi.org/10.1021/tx010022e, 2001.

Reda, A. A., Czech, H., Schnelle-Kreis, J., Sippula, O., Orasche, J., Weggler, B., Abbaszade, G., Arteaga-Salas, J. M., Kortelainen, M., Tissari, J., Jokiniemi, J., Streibel, T., and Zimmermann, R.: Analysis of gas-phase carbonyl compounds in emissions from modern wood combustion appliances: Influence of wood type and combustion appliance, Energ. Fuel., 29, 3897–3907, https://doi.org/10.1021/ef502877c, 2015.

Saraga, D., Maggos, T., Degrendele, C., Klánová, J., Horvat, M., Kocman, D., Kanduč, T., Garcia Dos Santos, S., Franco, R., Gómez, P. M., Manousakas, M., Bairachtari, K., Eleftheriadis, K., Kermenidou, M., Karakitsios, S., Gotti, A., and Sarigiannis, D.: Multi-city comparative PM2.5 source apportionment for fifteen sites in Europe: The ICARUS project, Sci. Total Environ., 751, 141855, https://doi.org/10.1016/j.scitotenv.2020.141855, 2021.

Schneider, E., Czech, H., Hartikainen, A., Hansen, H. J., Gawlitta, N., Ihalainen, M., Yli-Pirilä, P., Somero, M., Kortelainen, M., Louhisalmi, J., Orasche, J., Fang, Z., Rudich, Y., Sippula, O., Rüger, C. P., and Zimmermann, R.: Molecular composition of fresh and aged aerosols from residential wood combustion and gasoline car with modern emission mitigation technology, Environ. Sci.-Proc. Imp., 26, 1295–1309, https://doi.org/10.1039/D4EM00106K, 2024.

Steimer, S. S., Delvaux, A., Campbell, S. J., Gallimore, P. J., Grice, P., Howe, D. J., Pitton, D., Claeys, M., Hoffmann, T., and Kalberer, M.: Synthesis and characterisation of peroxypinic acids as proxies for highly oxygenated molecules (HOMs) in secondary organic aerosol, Atmos. Chem. Phys., 18, 10973–10983, https://doi.org/10.5194/acp-18-10973-2018, 2018.

Uski, O., Jalava, P. I., Happo, M. S., Torvela, T., Leskinen, J., Mäki-Paakkanen, J., Tissari, J., Sippula, O., Lamberg, H., Jokiniemi, J., and Hirvonen, M.-R.: Effect of fuel zinc content on toxicological responses of particulate matter from pellet combustion *in vitro*, Sci. Total Environ., 511, 331–340, https://doi.org/10.1016/j.scitotenv.2014.12.061, 2015.

Utinger, B., Campbell, S. J., Bukowiecki, N., Barth, A., Gfeller, B., Freshwater, R., Rüegg, H.-R., and Kalberer, M.: An automated online field instrument to quantify the oxidative potential of aerosol particles via ascorbic acid oxidation, Atmos. Meas. Tech., 16, 2641–2654, https://doi.org/10.5194/amt-16-2641-2023, 2023.

Vicente, E. D., Duarte, M. A., Calvo, A. I., Nunes, T. F., Tarelho, L., and Alves, C. A.: Emission of carbon monoxide, total hydrocarbons and particulate matter during wood combustion in a stove operating under distinct conditions, Fuel Process. Technol., 131, 182–192, https://doi.org/10.1016/J.FUPROC.2014.11.021, 2015.

Walgraeve, C., Demeestere, K., Dewulf, J., Zimmermann, R., and Van Langenhove, H.: Oxygenated polycyclic aromatic hydrocarbons in atmospheric particulate matter: Molecular characterization and occurrence, Atmos. Environ., 44, 1831–1846, https://doi.org/10.1016/J.ATMOSENV.2009.12.004, 2010.

Wang, S., Gallimore, P. J., Liu-Kang, C., Yeung, K., Campbell, S. J., Utinger, B., Liu, T., Peng, H., Kalberer, M., Chan, A. W. H., and Abbatt, J. P. D.: Dynamic Wood Smoke Aerosol Toxicity during Oxidative Atmospheric Aging, Environ. Sci. Technol., 57, 1246–1256, 2023.

Wong, J. P. S., Tsagkaraki, M., Tsiodra, I., Mihalopoulos, N., Violaki, K., Kanakidou, M., Sciare, J., Nenes, A., and Weber, R. J.: Effects of Atmospheric Processing on the Oxidative Potential of Biomass Burning Organic Aerosols, Environ. Sci. Technol., 53, 6747–6756, https://doi.org/10.1021/acs.est.9b01034, 2019.

World Health Organization: WHO global air quality guidelines. Particulate matter ($PM_{2.5}$ and PM_{10}), ozone, nitrogen dioxide, sulfur dioxide and carbon monoxide, WHO, 290 pp., ISBN 978-92-4-003421, 2021.

Wragg, F. P. H., Fuller, S. J., Freshwater, R., Green, D. C., Kelly, F. J., and Kalberer, M.: An automated online instrument to quantify aerosol-bound reactive oxygen species (ROS) for ambient measurement and health-relevant aerosol studies, Atmos. Meas. Tech., 9, 4891–4900, https://doi.org/10.5194/amt-9-4891-2016, 2016.

Zauli-Sajani, S., Thunis, P., Pisoni, E., Bessagnet, B., Monforti-Ferrario, F., De Meij, A., Pekar, F., and Vignati, E.: Reducing biomass burning is key to decrease $PM_{2.5}$ exposure in European cities, Scientific Reports, 14, 10210, https://doi.org/10.1038/s41598-024-60946-2, 2024.

Zhang, Z.-H., Hartner, E., Utinger, B., Gfeller, B., Paul, A., Sklorz, M., Czech, H., Yang, B. X., Su, X. Y., Jakobi, G., Orasche, J., Schnelle-Kreis, J., Jeong, S., Gröger, T., Pardo, M., Hohaus, T., Adam, T., Kiendler-Scharr, A., Rudich, Y., Zimmermann, R., and Kalberer, M.: Are reactive oxygen species (ROS) a suitable metric to predict toxicity of carbonaceous aerosol particles?, Atmos. Chem. Phys., 22, 1793–1809, https://doi.org/10.5194/acp-22-1793-2022, 2022.

Zhao, J., Zhang, Y., Sisler, J. D., Shaffer, J., Leonard, S. S., Morris, A. M., Qian, Y., Bello, D., and Demokritou, P.: Assessment of reactive oxygen species generated by electronic cigarettes using acellular and cellular approaches, J. Hazard. Mater., 344, 549–557, https://doi.org/10.1016/j.jhazmat.2017.10.057, 2018.